New UHV angle encoder for high resolution monochromators, a modern spare part for the Heidenhain UHV RON 905

F. Eggenstein*, L.Schwarz, T.Zeschke, J.Viefhaus
Department for Optics and Beamlines,

Helmholtz-Zentrum Berlin, Albert-Einstein Straße 15, D-12489 Berlin, Germany

*Corresponding author, email: frank.eggenstein@helmholtz-berlin.de

ABSTRACT

There are a large number of soft X-ray grating monochromators for high-resolution synchrotron radiation experiments in operation worldwide. At BESSY II eighteen of the monochromators currently in use are equipped with Heidenhain UHV RON905 angle encoders. Those angle encoders have successfully been in operation for decades. Today, this type of encoder has become a legacy product and repairs are getting expensive. Therefore, we have developed a new angle encoder, a mechanically compatible drop-in replacement of the RON905. A mechanically fitting prototype, based on RENISHAW absolute encoders, was tested on a high precision angle drive test bench. Fourier analysis of the encoder data allowed us to determine the precision for different angle ranges and indicates a better precision for the new angle encoder. Furthermore, we will introduce an on-line, in-situ method using electron/absorption spectroscopy to improve system accuracy with plane grating monochromators in collimated light using the newly developed encoder.

Keywords: XUV-radiation, plane grating monochromator, collimated light, angle encoder, synchrotron radiation

1. INTRODUCTION

Since the end of the 1990s, monochromators have been in operation to generate high-resolution soft X-Ray synchrotron radiation with the help of UHV high precision angle encoders. In this article we will discuss the relationship between radiation energy resolution and the necessary precision monochromator mechanics. We will mainly focus on plane grating monochromators in collimated light as they are widely used at BESSY and other synchrotron facilities. We will distinguish between angular encoder precision and system accuracy and why plane grating monochromators in collimated light are predestined to minimize the system accuracy of the encoder. This article addresses not only scientists but also engineers and technicians.

2. PLANE GRATING MONOCHROMATORS

In this chapter we will mention different designs of plane grating monochromators and specify helpful formulas. Monochromators for synchrotron radiation diffract light between the source and experiment by reflection gratings. The wavelength variation λ can physically be described with the grating equation

$$\lambda * N * m = (\sin(\alpha) - \sin(\beta)) \qquad \textbf{(1)}$$

Gratings with N equidistant lines per mm diffract the light in individual orders m, angle dependent between source and experiment, or alternatively, entrance and exit slit. Where α describes the incidence angle and β the exit angle to the normal of the deflected surface. The grating equation (1) differs from literature [1], but takes into account that β has a negative sign and the advantage is that we no longer have to consider this further. Synchrotron source and experiment are usually fixed and by rotating the grating at a fixed deflection angle 2θ

$$2\theta = \alpha + \beta \qquad \textbf{(2)}$$

, a change of the wavelength is simply possible.

In 1980 a complete description of plane grating monochromators in collimated light was published by Malcolm R. Howells [2]. His article considers aberration errors for spherical gratings, based on the standard theory [3] also known as optical path function [1], where the Rowland circle focusing condition is defined with:

$$C_{20} = \frac{1}{2}\left[\left(\frac{\cos(\alpha)^2}{r} - \frac{\cos(\alpha)}{R}\right) - \left(\frac{\cos(\beta)^2}{r'} - \frac{\cos(\beta)}{R}\right)\right] \quad \textbf{(3)}$$

Therefore, a fully focusing spherical grating with $C_{20} = 0$ and fixed entry and exit arms is fulfilled only at one wavelength by a correct set of all other variables. By considering a plane grating with R=infinite and a fully focusing system with $C_{20} = 0$, the result for the equation will directly written as

$$\frac{r'}{-r} = \left(\frac{\cos(\beta)}{\cos(\alpha)}\right)^2 = C_{ff}^2 \quad \textbf{(4)}$$

The important consequence of this equation is that, a fixed polychromatic source at distance r produce a fixed virtual monochromatic image behind the grating at distance r' simultaneously fulfilling the Rowland circle condition regardless of the wavelength keeping C_{ff} constant. The challenge of a constant C_{ff} is the necessary simultaneous change of the total deflection while the grating rotates. The first monochromator which solved this problem was named GLEISPIEMO [4].

In 1981, Helmuth Petersen and the company ZEISS invented the SX700 plane grating monochromator - a plane grating system where the virtual source at distance r' becomes a real image at the exit slit by using an elliptical mirror behind the grating. The special feature of this monochromator is the free change of the total deflection angle by using an eccentrically rotating plane mirror [5] [6] [7].

For the sake of completeness, it should also be mentioned, that at the same time various spherical grating monochromators were developed to meet the focusing requirements (3) for a larger wavelength range with the help of a plane mirror in the SX700 setup [8][9][10].

The first design of a SX700 plane grating monochromator in collimated light with the help of parabolic mirrors was developed in 1992 by G.Naletto, G.Tondello [11]. In 1997 Rolf Follath introduced an optical system with an SX700 plane grating monochromator mount equipped with RON905 UHV angle encoders (shown in Fig.1) in collimated light at BESSY II [12]. This System uses a toroidal pre mirror for collimation and a focusing cylindrical mirror behind the monochromator. Due to the parallel light the fixed parameter C_{ff} becomes variable and will now be designated as C_θ. Through this, higher orders can be simultaneous suppressed by freely selected total deflection angles [13] at a certain wavelength and the monochromator operates in both light directions.

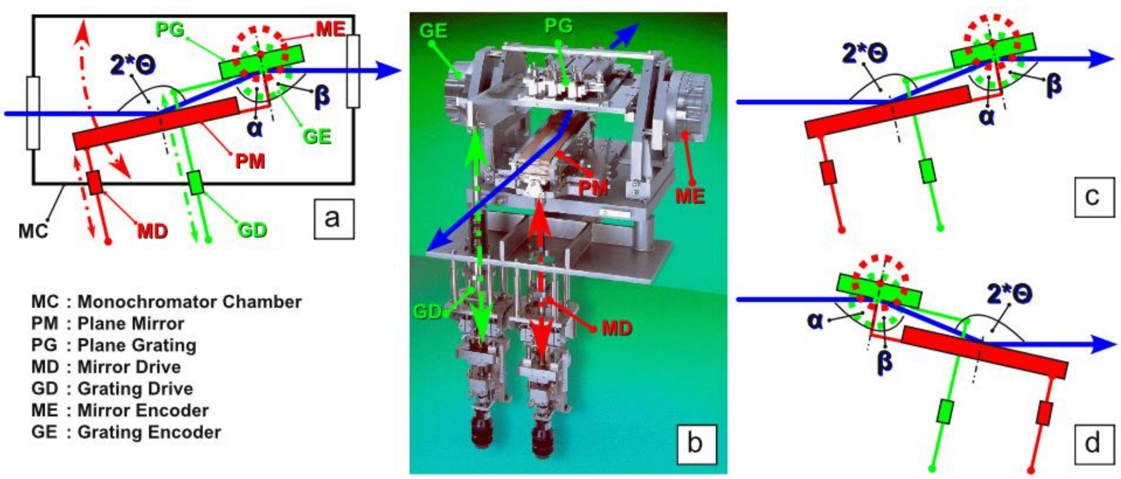

Figure 1 1b shows the mechanic of the BESSY II JENOPTIK monochromator, Graphic 1a illustrates the mechanic schematically. High precision linear drives rotate both optical elements via lever arm, while angle encoders simultaneously measure the angle change. The linear drive MD eccentrically rotates the mirror (red) in UHV. This is due to the synchrotron radiation deflects in the rotating axes of the plane grating. The linear drive GD rotates the grating (green) to diffract the light monochrome. Graphics 1c and 1d show the operation of the monochromator in both possible directions of incidence. 1c shows how polychromatic light is deflected from mirror to the grating. 1d outlines the case where diffracted light from the grating deflects by mirror where α becomes β and C_θ reciprocal.

3. PLANE GRATING MONOCHROMATOR SETTING

Only plane grating monochromators in collimated light will be considered in the following. The synchrotron community needs monochromatic photon energies E in eV and therefore, by using the Planck constant h and the speed of light c we mention the fundamental equation for transformation

$$\lambda = \frac{h * c}{E} \qquad \textbf{(5)}$$

For example, a photoionization spectrum of nitrogen needs photon flux at E=400 eV by a sufficient energy resolution. Therefore, a value of C_θ =2.5 with an available N=1200 l/mm grating in the first order m=1, is a good choice according to experience. From these parameters the angles for mirrors and gratings $\alpha, \beta, 2\theta$ can be calculated (see table 1 for an example) by a necessary additional formula:

$$\sin(\alpha) = \frac{\sqrt{\left(C_\theta^4 + C_\theta^2 * (\lambda * N * m)^2 - 2 * C_\theta^2 + 1\right)} - \lambda * N * m}{(C_\theta^2 - 1)} \qquad \textbf{(6)}$$

Formula (6) is derived from formulas (1) and (2) by the application of trigonometric Pythagoras and the use of binomial formulas.

Table 1. Photon energy setting at 400eV

Experiment Setting			Monochromator Setting		
E	=	400eV	λ	=	3.099 nm
N	=	1200 l/mm	α	=	87.845°
C_θ	=	2.5	β	=	84.607°
m	=	1	2θ	=	172.453°

4. ANGLE ENCODERS AND HIGH ENERGY RESOLUTION

High precision encoders are necessary to generate high resolution synchrotron radiation with grating monochromators. In the following we will discuss this in the context of error propagation. The JENOPTIK and SX700 type monochromators both have two axes, one for grating rotation and one for the eccentrically mirror rotation. Therefore, the grating equation can be expressed using either as a sum or as a product formula

$$\lambda = (\sin(2\theta - \beta) - \sin(\beta))\frac{1}{N * m} = 2\cos(\theta)\sin(\theta - \beta)\frac{1}{N * m} \qquad \textbf{(7)}$$

The wavelength changes by turning the mirror θ and grating β. Angular perturbations and angular misalignments during adjustment can lead to a deviation of the wavelength, which is considered below with the variance formula. [14].

$$\Delta\lambda = \sqrt{\left(\frac{\delta\lambda}{\delta\beta}\right)^2 * \Delta\beta^2 + \left(\frac{\delta\lambda}{\delta\theta}\right)^2 * \Delta\theta^2} \qquad \textbf{(8)}$$

$$\Delta\lambda = \sqrt{\left(2\cos(\theta)\cos(\beta - \theta) * \frac{1}{N * m}\right)^2 * \Delta\beta^2 + \left(2\cos(2\theta - \beta) * \frac{1}{N * m}\right)^2 * \Delta\theta^2} \qquad \textbf{(9)}$$

Consequentially, we can express the expected resolution R due to the angular perturbations with

$$R = \frac{\lambda}{\Delta\lambda} = \frac{E}{\Delta E} \qquad \textbf{(10)}$$

Using the physical quantities from table 1, table 2 show exemplarily the results of error propagation with angular perturbations of 1” at the monochromator setting C_θ =2.5 and the reciprocal $C_\theta = 1/2.5 = 0.4$

Table 2. Error propagation results at 400eV

$E = 400\text{eV}, \lambda = 3.099\text{nm}$, $\Delta\beta = 1'', \Delta\theta = 1'', [1'' = 1\ \text{arcsec}]$							
C_θ	β	2θ	$\frac{\delta\lambda}{\delta\beta} * \Delta\beta$	$\frac{\delta\lambda}{\delta\theta} * \Delta\theta$	$\Delta\lambda$	R	ΔE
2.5	84.607°	172.452°	0.0005 nm	0.0003 nm	0.0006 nm	5165	77meV
0.4	87.845°	172.452°	0.0005 nm	0.0007 nm	0.0009 nm	3443	116meV

The reciprocal of $C_\theta = 1/2.5 = 0.4$ causes an exchange of α and β. Because the rate of the grating deviation remains, the rate of the mirror deviation increases for $C_\theta = 0.4$. For an operation of plane grating monochromators in collimated light this has the consequence that, light is deflected from mirror to grating configuration (see figure 1c). Therefore, in this case a selection of $C_\theta > 1$ will increase the resolution. Inversely (see figure 1d) if light is deflected from grating to mirror, the resolution will only increase by a selection of $C_\theta < 1$, while $C_\theta = 1$ corresponds to the zeroth order where $\lambda = 0$ and the light will be polychromatic at the exit as well. The dependence of the energy resolution is depicted in figure 2 over a wide energy range at different C_θ for an angular perturbation of $\Delta\theta = 1''$ and $\Delta\beta = 1''$ for the configuration outlined in figure 1c.

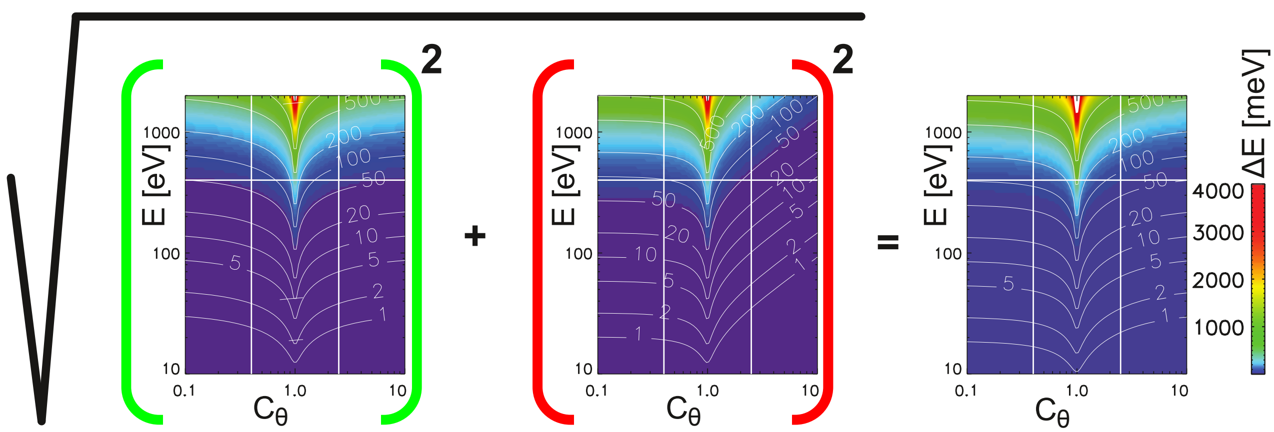

Figure 2 Energy deviation, caused by an angular perturbation of $\Delta\beta = 1''$ and $\Delta\theta = 1''$. From left to right, the green brackets represent the energy deviation of the grating, the red brackets represent the deviation of the mirror and the sum of energy deviation. The horizontal white line marks the energy at 400 eV and the vertical lines indicates the two different C_θ values from the examples given in table 2.

Finally, if only the resolution is considered, a formula independent of the line density N and order m can be derived:

$$R = \frac{\lambda}{\Delta\lambda} = \frac{2\cos(\theta)\sin(\theta - \beta)}{\sqrt{(2\cos(\theta)\cos(\beta - \theta))^2 * \Delta\beta^2 + ((2 * \cos(2\theta - \beta))^2 * \Delta\theta^2}} \tag{11}$$

The result for 1” angular perturbations of $\Delta\theta$ and $\Delta\beta$ are presented in figure 3.

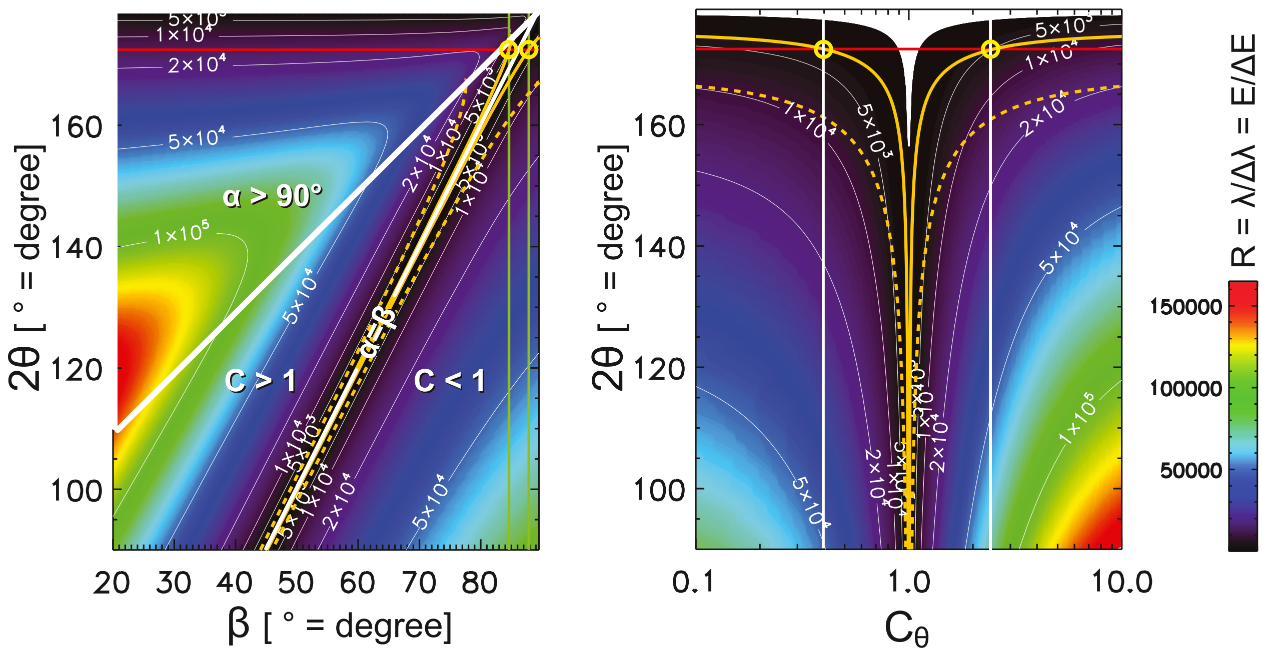

Figure 3 The resolution R caused by the mirror and grating drives for an error deviation $\boldsymbol{\Delta\theta}$ and $\boldsymbol{\Delta\beta}$ of 1”, respectively. The result is independent of line number N and order m. The white framed triangle in the graph on the left side indicates a calculated resolution but a not defined setting of a reflection grating. The yellow circles mark both C_θ values of table 2. The white line $\boldsymbol{\alpha = \beta}$ in between presents the zero order, defined by $C_\theta = 1$. The solid and dotted yellow lines, identifies the line of constant energy. By using a 1200l/mm Grating in first order describes the solid line E=400eV and the dotted E=64eV. On the right side the dependence of the total deflection angle on the C_θ value is shown. The graph serves to better illustrate the lines of constant energy and establish a relation to a plane grating monochromator setting.

The mathematical relation between the precision of the angle adjustment and the energy resolution of an SX700-type plane grating monochromator mount is done by the help of the error propagation variance formula. An angular perturbation of 1" was considered, resulting in a resolution of R=5165 at 400eV. In order to display a photoionization spectrum of nitrogen gas at 400eV with high resolution, an energy resolution of about R=10000 is required [15] From this fact, the JENOPTIK-type monochromators were equipped with high-precision drives and UHV HEIDENHAIN RON905 angle encoders to ensure angle adjustments in the sub-second range [16].

5. A NEW ANGLE ENCODER AS A SPARE PART FOR THE RON905

The UHV RON905 has been in use for decades. However, repairs are becoming more difficult and expensive. The same applies to the associated electronic hardware. For this reason, a new encoder, shown in figure 4, was developed in-house. The new RON905 spare part was designed such that it can easily replace the existing RON905 encoders in use at eighteen existing monochromators at BESSY II. The construction consists of a rotor and a stator, which were equipped with RENISHAW absolute readout components. The challenge was to completely change the encoder systems without having to rebuild the existing monochromator mechanics. As a positive additional feature, the use of absolute encoders makes a complicated reference run after a power shutdown of the monochromator unnecessary.

In the design solution presented here, the four individual RENISHAW read heads provide absolute angle values directly in the BISS-C protocol. Two read heads are mounted diametrically opposite each other and compensate for the effects of bearing play and eccentricity. The pairs of read heads are rotated by 90° and form the total angle value by averaging.

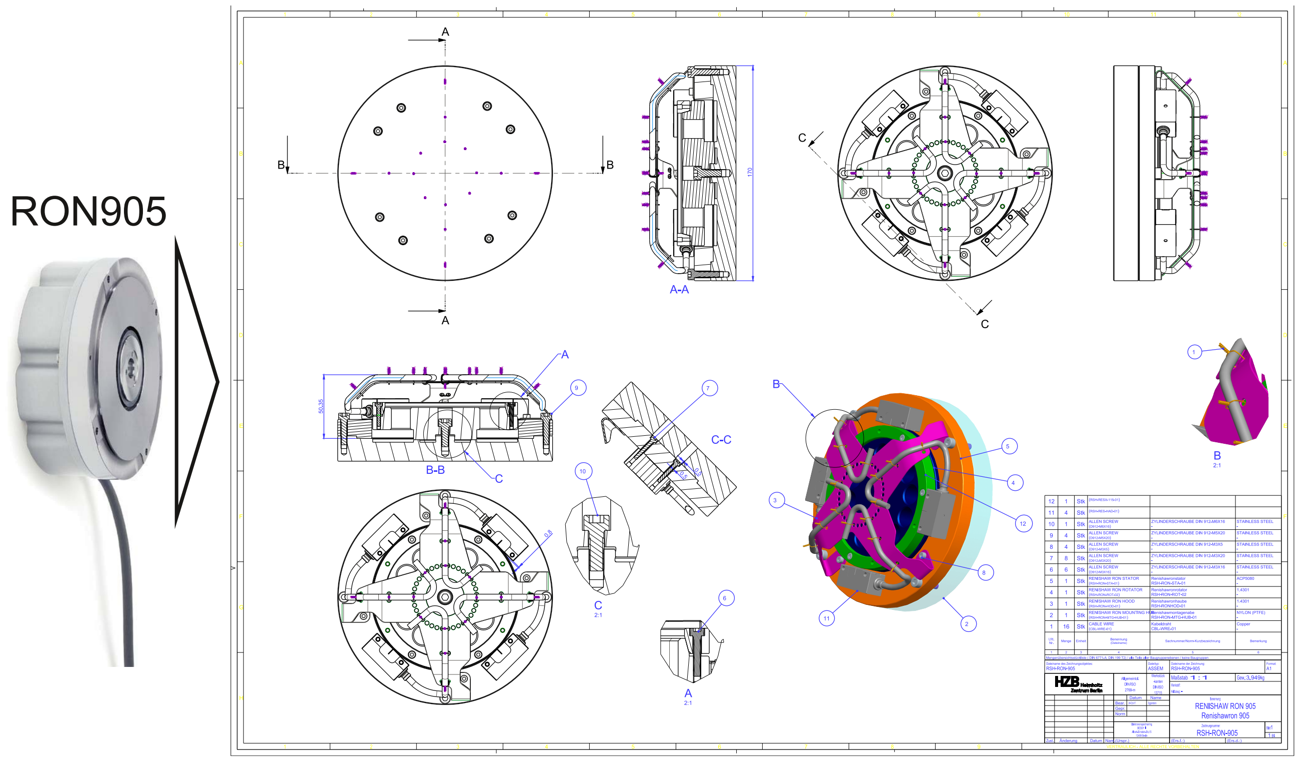

Figure 4 The angle encoder RON905 from HEIDENHAIN on the left side is a self-contained system, which is fitted to the mirrors or grating axes with several screws. The solution of the newly developed encoder system on the right side uses the same mounting points and dimensions and consists out of two parts, a rotor and a stator. The rotor is used to hold the RENISHAW absolute scale ring, while the stator has the associated four read heads to determine the absolute angle change, see also Figure 5.

The manufactured prototype has been tested on a high precision angle encoder test bench, shown in figure 5. A lever arm, driven by high precision linear drive with spindle, rotates the angle encoder. The linear drive, shown in in table 4.1, is equipped with gears and has a micro step operation working stepper motor for the reduction ratio.

The test bench was specially designed for RENISHAW absolute angle encoders with two read heads and a REXA 255mm in diameter absolute scale code marked ring, in the following named REXA255. The main objective in using this test bench was to compare and calibrate an REXA255 encoder and an RON905 encoder. The REXA255 system with better accuracy and higher resolution (as specified by the manufacturer) could not serve as a direct replacement of the RON905, due to its larger dimensions and the lack of installation space.

Our in-house developed solution with four read heads and a smaller and low-cost RESA 115mm in diameter absolute scale code marked ring, following as RESA115 designated, was measured on the same test bench.

The measurements were taken to estimate whether the RESA115 system could also compete with the precision of the RON905 system. The extensive series of tests was initially carried out with both RON905 and REXA255 systems at the same time. In a second series of tests, the RON905 was replaced by the RESA115 system. The REXA255 encoder system data served as an intermediary between the systems RON905 and RESA115.

Table 3 Angle encoder comparison, catalog data.

Name	RON905	REXA255 (2 HEAD)	RESA115 (4 HEAD)
Acurracy 360° rotation	± 0.4“	± 1.11“ (Ø255mm)	± 2.44“ (Ø115mm)
Grating period	36“± 0.3“	48.5“± 0.06“(30µm ± 40nm)	107.6“± 0.14“(30µm ± 40nm)
Approx. costs (2019)	15000€	6000€	5000€

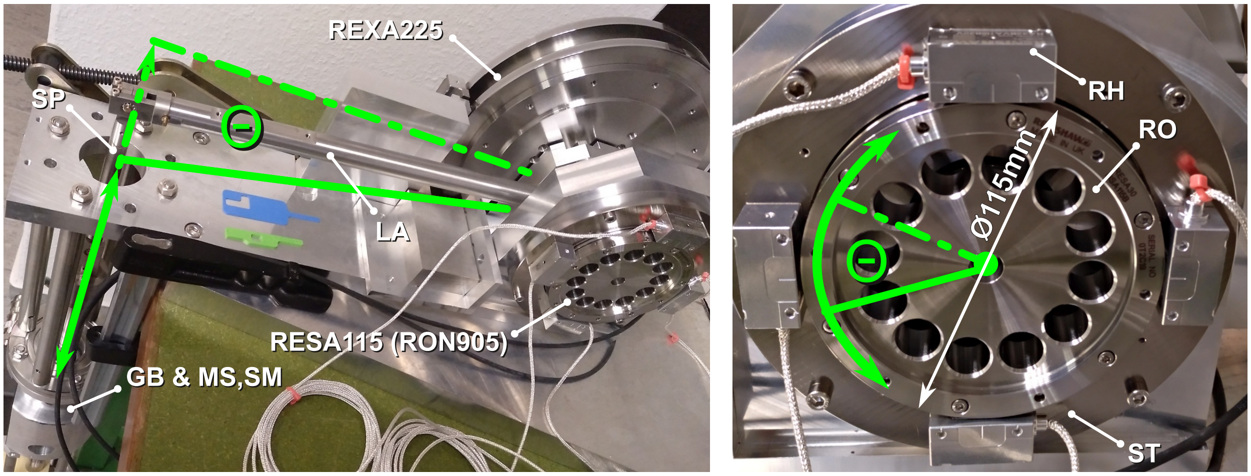

Figure 5 The test bench for high precision angle movements. A stepping motor (SM) in micro stepping mode (MS) drives a spindle (SP) via a gearbox (GB) and moves a lever arm (LA) into rotation. The picture shows the exchanged RESA115 with an Ø115mm Rotor (RO) and four read heads (RH) mounted on a stator (ST). The data of two angle encoders have been simultaneously measured, while the high-precision drive performs an angle change.

Table 4 Test bench hardware parameters and measurement series

4.1 Test bench performance		
$-18° < \Theta < 2{,}3°$		
LA	Lever arm	396mm
SP	Spindel pitch	0.5mm/rev
GB	Gearbox	1/50
SM	Stepping motor	400step/rev
MS	Micro stepping	1step/512
$\Delta\Theta = \arctan\left(\frac{SP}{LA} * \frac{GB}{SM * MS}\right) = 25'' * 10^{-6}$		

4.2 Angle encoder measurement series 1” = 1arcsec				
	$\Delta\Theta = \Theta_{REXA255} - \Theta_{RON905}$		$\Delta\Theta = \Theta_{REXA255} - \Theta_{RESA115}$	
No.	Θ	$d\Theta/dt$	Θ	$d\Theta/dt$
1	$-18° \rightarrow 2.3°$	180"/s	$-18° \rightarrow 2.3°$	180"/s
2	$0° \rightarrow -0.22°$	2"/s	$0° \rightarrow -0.22°$	2"/s
3	$-1.13° \rightarrow -0.91°$	2"/s	$-1.13° \rightarrow -0.91°$	2"/s
4	$-15° \rightarrow -14.78°$	2"/s	$-15° \rightarrow -14.78°$	2"/s

Four different angle ranges have been measured to compare the performance of the RON905 and the RESA115. The angle ranges are summarized in table 4.2. In the measurement No. 1, the whole possible angle range of 20.3° = 73080” was measured. More accurate measurements in the range of 0.22° = 800" have been done in measurement No. 2-4. Where No.3 represent the range, where the lever arm is close to horizontal.

The Data was generated with a sampling rate of 9 Hz for each encoder simultaneously. The measured angle data was then subtracted, respectively. The remaining deviation, REXA255-RON905 and REXA255-RESA115, results in a value which contains systematic and random uncertainties (including system noise). This result was further quantitatively investigated and analyzed via power density spectrum.

The power density spectra have been generated by a Fourier transformation of the difference signal into harmonic power oscillations per bandwidth $1/\Theta$. By integration of harmonic oscillations backwards from small spatial frequency to large spatial frequency, or respectively the square root of the reverse running integral PSD, the data could be compared and analyzed for the relevant investigated angle range.

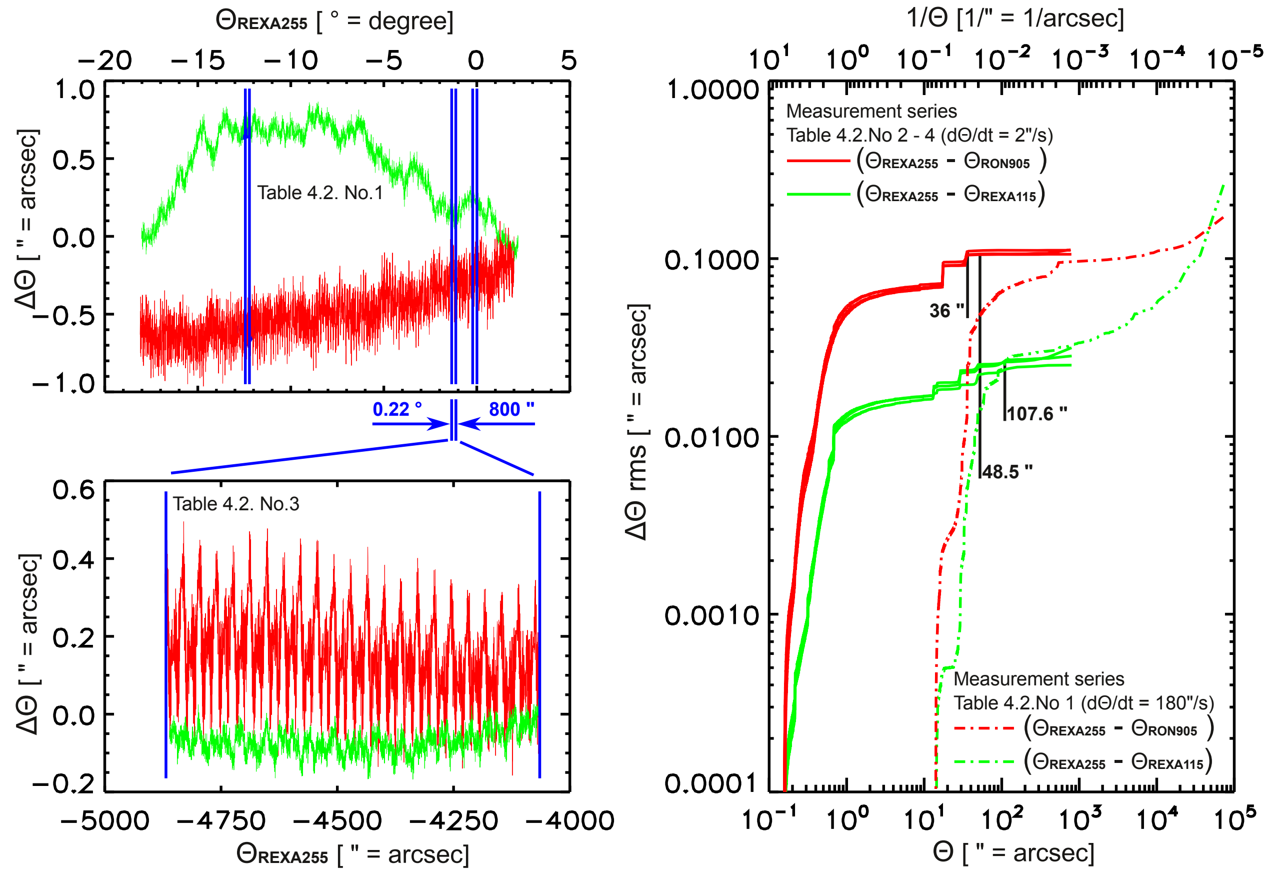

Figure 6 On the left side the difference signal ΔΘ of Table 4.2, formed from the subtraction of the correspondingly two angle encoder measured data. At the top measurements in the whole angular test bench range of 20.3°, respectively 73080”, with a measuring frequency of 180”/s are shown. At the bottom one of the 3 different measured regions in a range of 800” with a measuring frequency of 2”/s is depicted. On the right side, the backwards integrated power density spectra given in order to analyze the data of all measurements. The three grating periods of the angular encoders from table 3, 36", 48.5" and 107.6" are drawn as vertical lines. As an example, in a 3eVenergy scan at 400eV with a $C_\theta = 2.5$ setting, rotates the mirror 50” and the grating 70”. The encoder precision of such a scan corresponds to 0.1” by using the RON905 and 0.02" using the new encoder RESA115.

6. INCREASING SYSTEM ACCURACY

The precision of the angle encoders could be determined with the measurements on the test bench presented above. The results show a higher precision for the RESA115 in comparison with the RON905. Precision is not the same as accuracy and the effect of missing accuracy can be displayed by measured nitrogen spectra at different C_θ values. According to the present results, it can be determined that the precision or resolution is reached indeed. Comparison of the individual measurement, as illustrated in figure 7 by two nitrogen spectra, supports the initial assumption that the energy scale is shifted, stretched or compressed. This is a result from the uncertainties of the angle encoder system. Using measurements based on synchrotron radiation in order to increase the system accuracy provides an in-situ method for calibration. The monochromator is used to excite inner-shell electrons in nitrogen gas, for which the transition energies are known quite precisely [17]

For a known and calibrated angle θ of the plane mirror and a given photon energy, the angle for the plane grating can be determined due to the product formula (7)

$$\beta = \theta - \arcsin\left(\frac{\lambda * N * m}{2\cos(\theta)}\right) \quad \textbf{(12)}$$

Vice versa, due to the sum formula (7), by a fixed angle β on the grating, the mirror can be used for energy scanning, by

$$2\theta = \arcsin(\lambda * N * m + \sin(\beta)) + \beta \quad \textbf{(13)}$$

This allows a calculation of the angle changes either for the grating or mirror for an energy scan.

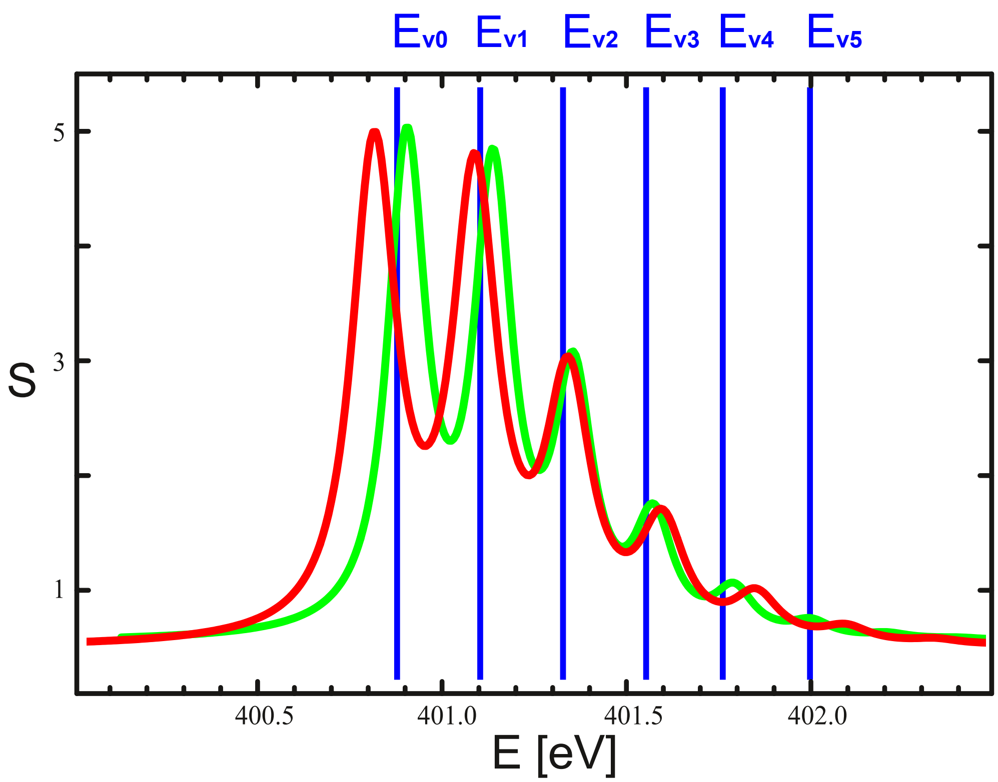

Figure 7 illustrates the difference between resolution and accuracy by the example of a nitrogen ionization spectrum. The resolution can be determined from the signal height S of individual excitation energies Ev0-Ev5 [17]. The red curve represents a measurement with a different C_θ value. The resolution is equal but shifted energetically. The aim of the calibration method is to bring the spectra with different C_θ values to coincidence.

By the help of formula (12), (13) the monochromator has to be controlled such, that it scans energetically between two known energy states simultaneously measuring the angle of the encoder for the respective optical element. The scan with the grating is started with a fixed, calibrated and known mirror position θ. The measured value of the grating encoder will then be calibrated with the calculated value. The mirror is then used at the new position of the grating to scan the mirror backwards to the beginning energy state. In this way, if the scan is repeated frequently, a large angle range of the respective encoder can be calibrated.

This overall procedure is underlined by a flowchart in figure 8. In the flowchart, the scanning is done with the grating from the first maximum of the nitrogen excitation to the first minimum with decreasing angle differences until the continuous signal S change reverses. Subsequently, the scanning is done in the same way with the mirror from minimum to maximum and so on, until the maximum possible angular range of the monochromator is reached by limit switch. During the alternate scan with mirror and grating the angles are calibrated on the encoder. Both encoders move along the yellow line at 400eV in figure 3 for this particular energy scan. To cover larger angle areas of the encoder with ionization spectra, other inert or noble gases can be used, e.g. helium [15] around a photon energy of 64eV. See also the dotted yellow line of constant energy for 64 eV in figure 3.

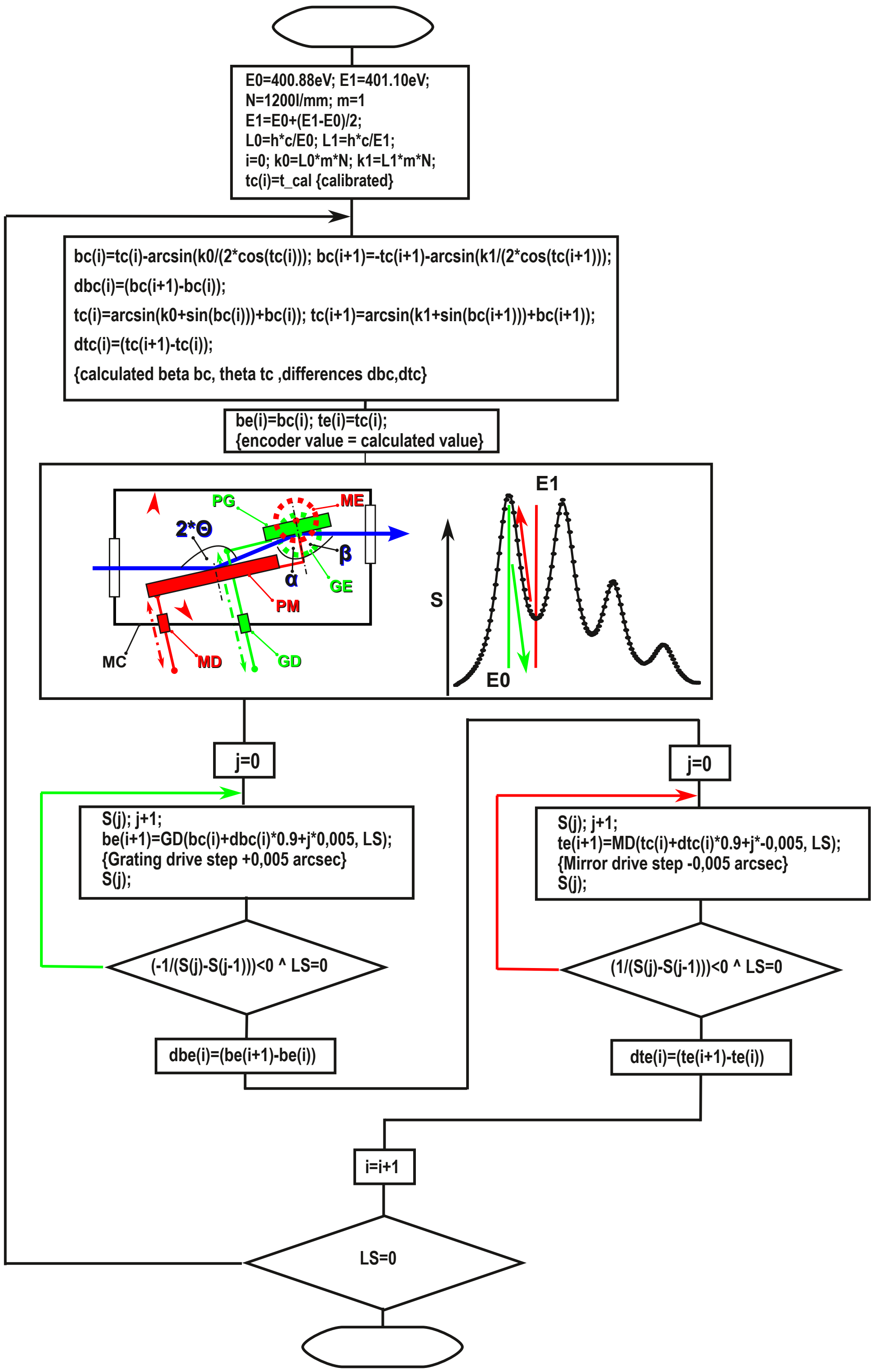

Figure 8 The computer flow chart to increase the accuracy of the angle encoders in situ

7. CONCLUSION AND OUTLOOK

We discussed the influence of angular encoders typically employed in a soft X-ray monochromator on the energy resolution with the help of the error propagation. We give an example for 1” deviation of the optical elements involved. Further measurements have been performed on a test-bench and allowed to determine the precision of different angle encoders.

The measured data shows that the RESA115 system not only fits the installation space, but that the systems RON905 and RESA115 show at least similar uncertainties and are therefore directly interchangeable. The RESA115 system has even demonstrated a better resolution than the RON905 system. In addition to that, the absolute encoder system ensures that a reference run is no longer necessary after the system has been powered off.

In contrast to the analog signals of the RON905 system, the RESA115 encoders provide digital signals. The old and expensive electronics for converting the signals are no longer needed and computer readouts are therefore much easier.

Using the available results, the drive chain of the monochromator drive can be further optimized. The drive chain in tabular 4.1 on the test stand is $\Delta\Theta' = 25'' * 10^{-6}$. The micro stepping method could be adapted or even omitted to increase angular velocity and thus shorten time taken up for energy scans.

We presented an in-situ method which increases accuracy, although it has to be conceded that the method requires further additional testing on a monochromator equipped with RESA115 encoder systems.

An optics laboratory is currently being set up at BESSY II to develop ex-situ methods for the adjustment of monochromators with geodetic instruments. The calibration of the optical elements to the absolute encoder is of great importance here. As shown in the calibration process flowchart, the initial angle θ must be determined very accurately.

Before installing a plane grating monochromator on the storage ring, the optical elements should be calibrated by the use of a high accuracy electronic autocollimator. Just as with the alternating movement of the optical elements in the flow chart in figure 8, between two energy states, a parallel movement can be performed by autocollimator measurements. The measured angle values of the respective encoder can be calibrated by the autocollimator measured data [18]. The aim is to calibrate the optical elements to the absolute encoders and further to increase the accuracy of the whole system prior to installation.

REFERENCES

[1] X-Ray Data Booklet Section 4.3 Gratings and Monochromators
[2] Malcolm R. Howells Nuclear Instruments and Methods 177 (1980)127-139
[3] M.V.R.K. Murty, J.O.S.A. 52 (1962) 7,768
[4] C. Kunz et al., J. Opt. Soc. Am. 58 (1968) 1415
[5] H. Petersen, Opt. Comm. 40 (1982) 402
[6] A.V. Pimpale, S.K. Deshpande, V.G. Bhide, Appl. Opt. 30(1991) 1591
[7] F. Riemer, R. Torge, Nucl. Instr. and Meth. 208 (1983) 313
[8] H.Padmore Review of Scientific Instruments **60**, 1608 (1989)
[9] F.Senf et al. Review of Scientific Instruments 63, 1326 (1992)
[10] W.B. Peatman et al., Review of Scientific Instruments 66 (1995) 2801
[11] G.Naletto, G.Tondello Pure Appl. Opt. 1 347 (1992)
[12] R.Follath, F.Senf Nuclear Instruments and Methods in Physics Research A 390 (1997) 388-394
[13] R.Follath, Nuclear Instruments and Methods in Physics Research A 467–468 (2001) 418–425
[14] H. H.Ku, Journal of Research of the National Bureau of Standards. 70C (4): 262 (1966).
[15] S.I. Fedoseenko et al. Nuclear Instruments and Methods in Physics Research A 505 (2003) 718–728
[16] F.Senf et al, J. Synchrotron Rad.(1998).5, 584±586
[17] Rana N.S.Sodhi, C.E.Brion, J. of Electron Spectroscopy and Related Phenomena, Vol. 34, Issue 4, 1984, 363-372
[18] F.Eggenstein, F.Radu, Patent pending DE102018100603A1, 2018